Earth Syst. Sci. Data, 18, 3833–3852, 2026
https://doi.org/10.5194/essd-18-3833-2026
© Author(s) 2026. This work is distributed under
the Creative Commons Attribution 4.0 License.

Open Access Earth System Science Data

The GSFC Lidar Observation and Validation Experiment (GLOVE) field campaign

John E. Yorks[1], Edward P. Nowottnick[1,2], Steven Platnick[1], Kerry G. Meyer[1], Matthew Walker McLinden[1], Meloe S. F. Kacenelenbogen[1], Kenneth E. Christian[3], Joseph A. Finlon[3], Natalie A. Midzak[1], Natalia Roldán-Henao[4], Patrick A. Selmer[3], Matthew J. McGill[5], Erica K. Dolinar[6], Charles N. Helms[3], Robert Koopman[7], Jonas von Bismark[7], and Montserrat Piñol Solé[7]

[1]NASA Goddard Space Flight Center, Greenbelt, MD, USA
[2]NASA Headquarters, Washington, DC, USA
[3]Earth System Science Interdisciplinary Center, University of Maryland College Park, College Park, MD, USA
[4]Department of Atmospheric and Oceanic Sciences,
University of Maryland College Park, College Park, MD, USA
[5]Department of Chemical and Biochemical Engineering, University of Iowa, Iowa City, IA, USA
[6]US Naval Research Laboratory, Marine Meteorology Division, Monterey, CA, USA
[7]European Space Agency, ESA – ESTEC, Noordwijk, the Netherlands

Correspondence: John E. Yorks (john.e.yorks@nasa.gov)

Received: 18 December 2025 – Discussion started: 9 March 2026
Revised: 8 May 2026 – Accepted: 12 May 2026 – Published: 4 June 2026

Abstract. The Goddard Space Flight Center's Lidar Observation and Validation Experiment (GLOVE) was a field campaign conducted from 27 January to 28 February 2025, based out of NASA Armstrong Flight Research Center at Edwards Air Force Base in California. Its main goals were to validate atmospheric data products from the Ice, Cloud, and Land Elevation Satellite-2 (ICESat-2) and the Earth Cloud, Aerosol and Radiation Explorer (EarthCARE) satellite missions. The campaign utilized NASA's high-altitude Earth Resources-2 (ER-2) aircraft, equipped with four remote sensing instruments – including two lidars, a radar, and a spectrometer. GLOVE carried out eight flights totaling 40 flight hours and successfully captured seven ICESat-2 and six EarthCARE underflight segments of varying atmospheric conditions (i.e., aerosols, cirrus, and stratocumulus clouds) and surface types. The data collected during ICESat-2 underflights, especially of cirrus clouds and aerosols, offer valuable opportunities to assess the performance of both the operational and newer research-grade atmospheric ICESat-2 data products during daytime. Notably, the data from the Cloud Radar System (CRS), especially from snow-producing clouds, will play an important role in understanding the potential errors and uncertainties in EarthCARE Cloud Profiling Radar (CPR) Doppler data, the first-ever radar Doppler velocity measurements from space. All GLOVE data products are publicly accessible through a NASA Distributed Active Archive Center (DAAC) or other free, open-access repositories (please see Sect. 4, "Data availability", for the DOIs and full data set citations). GLOVE serves as an example for conducting cost-effective and efficient airborne satellite validation campaigns.

Published by Copernicus Publications.

1 Introduction

Clouds and aerosols play a significant role in determining the overall atmospheric radiation budget yet remain a key uncertainty in understanding the Earth's atmosphere. Aerosols affect the top-of-atmosphere (TOA) radiation budget by reflecting and absorbing sunlight (Haywood and Boucher, 2000), and indirectly by interacting with clouds (Twomey, 1977; Albrecht, 1989; Ackerman et al., 2000; Rosenfeld et al., 2001). Aerosols from volcanic eruptions, wildfires, and dust storms are also hazardous to aviation safety and human health (Mathur, 2008; Miller et al., 2011; Colette et al., 2011). Ice clouds can induce a significant daytime TOA warming effect (Ackerman et al., 1988; McFarquhar et al., 2000; Stephens, 2005), while liquid water clouds cause a large corresponding cooling effect (Rajeevan and Srinivasan, 2000). These impacts on the Earth system remain a key uncertainty, requiring spaceborne lidar, radar, and spectrometer sensors, among others, to accurately observe the spatiotemporal variability of clouds and aerosols, especially over the oceans and remote land areas that are difficult to access.

In 2025, there are only two satellite missions that provide vertical profiles of clouds and aerosols via publicly available data products: the Earth Cloud, Aerosol and Radiation Explorer (EarthCARE) satellite mission implemented by the European Space Agency (ESA) and Japan Aerospace Exploration Agency (JAXA), and the Ice, Cloud, and Land Elevation Satellite-2 (ICESat-2) mission implemented by NASA GSFC. EarthCARE, launched in 2024, is designed to study the interactions between clouds, aerosols, and radiation in the Earth's atmosphere (Illingworth et al., 2015), with the primary goal of characterizing clouds and aerosols, including their properties, vertical structures, and interactions with radiation using a suite of four instruments: a high spectral resolution lidar (HSRL), a cloud radar, a shortwave (SW) and longwave (LW) broad-band radiometer, and a multi-band SW/LW spectrometer. The Ice, Cloud, and Land Elevation Satellite-2 (ICESat-2) mission was launched in 2018, primarily to provide high-resolution altimetry data of the Earth's surface and cryosphere (Markus et al., 2017). A secondary goal of the ICESat-2 mission is to measure cloud and aerosol layer heights and optical properties, especially in the polar regions. The main instrument is the Advanced Topographic Laser Altimeter System (ATLAS), which includes an atmospheric channel that provides 532 nm backscatter profiles from 0–14 km altitude at 280 m horizontal and 30 m vertical resolution using 3 strong laser beams (532 nm), each 3 km apart across track at the surface (Palm et al., 2021).

Validation of satellite remote sensing data from missions like ICESat-2 and EarthCARE is crucial for understanding the limitations, accuracies, and reliability of the data. Typical validation studies involve comparing spaceborne data products with a "truth" dataset, such as ground or aircraft measurements with higher accuracy and/or finer resolutions. EarthCARE data products were released starting late 2024 and ESA's validation activities have begun accordingly, including 15 campaigns for a total of 127 underflights in 2024 and 2025. As part of the EarthCARE validation team (ECVT), these activities have been coordinated by ESA and the EarthCARE Date Innovation and Science Cluster (DISC), enabling scientists to collaborate with the mission's algorithm and instrument experts. Operational ICESat-2 atmospheric data products have been publicly available since 2018, but validation activities have been limited to 2 aircraft flights in 2019 (Palm et al., 2021) and comparisons to other spaceborne sensors (Christian et al., 2025). Additionally, a new ICESat-2 atmospheric research data product is being developed that includes machine learning techniques (Gomes et al., 2025). More validation of the EarthCARE and ICESat-2 cloud and aerosol data products is required to further understand the range of potential errors and uncertainties associated with these products, allowing users to appropriately use the data and make more informed interpretations.

The Goddard Space Flight Center (GSFC) Lidar Observation and Validation Experiment (GLOVE) was a field campaign that took place from 27 January to 28 February 2025 out of NASA's Armstrong Flight Research Center at Edwards Air Force Base in California. The objectives of GLOVE were to: (1) validate new ICESat-2 atmospheric data products, (2) validate EarthCARE lidar, radar, and spectrometer data products, and (3) test a new airborne lidar laser alignment. GLOVE flew 4 satellite simulating remote sensing instruments on the high-altitude NASA ER-2 aircraft (Fig. 1):

- Cloud Physics Lidar (CPL)
- Roscoe Nadir/Zenith Lidar
- Cloud Radar System (CRS)
- Enhanced MODIS Airborne Simulator (eMAS)

A total of 13 satellite underflight segments (20–40 min each) were performed during 8 aircraft flights over various atmospheric scenes (aerosols, cirrus clouds, stratocumulus clouds, etc.) and surface types (ocean, land, mountains, etc.). All the GLOVE data products are freely available at a NASA Distributed Active Archive Center (DAAC) or other free, open-access repositories (Sect. 4). This paper will describe the GLOVE objectives and the four instruments flown, detail the operations during the campaign, and summarize all the science flights from the campaign.

2 Objectives

2.1 ICESat-2 Validation

ICESat-2 is the successor to the original ICESat mission and has been operating continuously since October 2018 (Markus et al., 2017). While it was specifically designed to provide high-resolution altimetry data of Earth's surface,

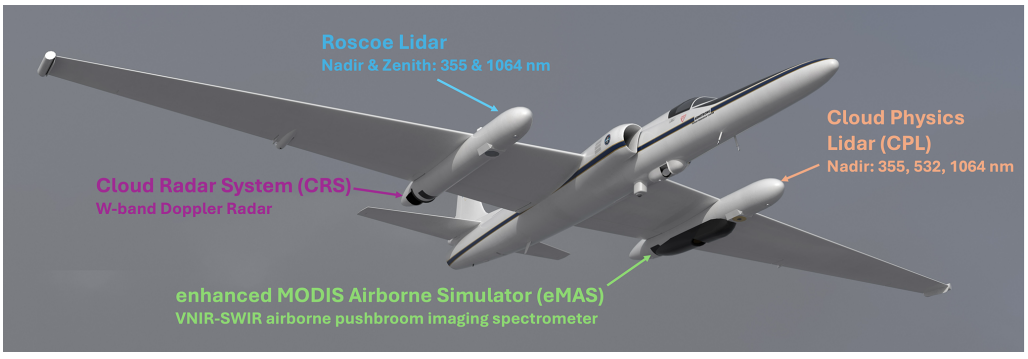

Figure 1. Schematic that shows the physical location of the CPL, Roscoe, CRS, and eMAS sensors on the NASA ER-2. This schematic was created by annotating a NASA Airborne Science Program 3D model of the ER-2 (https://airbornescience.nasa.gov/3d-models/, last access: 27 May 2026).

ICESat-2 is also equipped with an atmospheric channel capable of detecting backscatter from clouds and aerosols between 14 km altitude and the surface. ATLAS, the only instrument aboard the satellite, uses a 532 nm laser operating at a high pulse rate (10 kHz) with low energy per pulse (500 µJ), along with photon-counting detectors (Table 1). ATLAS employs a diffractive optical element (DOE) to split each laser pulse into six beams. Of these, three are classified as "weak beams" with about 25 µJ per pulse, and the other three as "strong beams" with roughly four times the energy. All six beams are used for surface elevation measurements, but only the three strong beams – labeled "profile1", "profile2", and "profile3" in the ATL04 and ATL09 data products – are used to gather atmospheric backscatter profile data. These atmospheric backscatter profiles span a vertical column of 14 km, divided into 30 m bins. Typically, this column ranges from about 13.75 km above the local surface elevation (based on the onboard Digital Elevation Model) to −0.25 km below it. For atmospheric observations, the three strong beams are downlinked after averaging 400 laser shots onboard, yielding three 25 Hz profiles with a spatial resolution of 280 m along the satellite's track (Palm et al., 2021).

The operational atmospheric data product (ATL09) provides three calibrated attenuated backscatter profiles (one for each of the three "strong" beams), in the 532 nm wavelength along with layer identification, layer top and bottom altitudes, cloud/aerosol discrimination, and column optical depth, among other variables, at 25 Hz (∼ 280 m horizontal) by 30 m vertical resolution. In the standard product (v006), cloud and aerosol layer heights and discrimination are determined using a density dimension algorithm (DDA), which uses a moving window, corresponding to ∼ 12 profiles (3 km), to detect areas with scattering exceeding background levels within the profile (Palm et al., 2021). Compared to space-based lidars designed primarily for atmospheric observations, ATLAS has some shortcomings including (1) poor daytime signal-to-noise ratio (SNR), (2) a high repetition rate (10 kHz), which limits the ATL09 data frame to 14 km above the ground and can cause signals from above 14 km to be "folded" down into the lower troposphere (Christian et al. 2025), and (3) a lack of linear depolarization, which complicates cloud/aerosol discrimination and feature subtyping. Christian et al. (2025) showed that while cloud detections in the current ICESat-2 data products generally agreed with those observed by the CALIOP lidar at night, daytime cloud and all aerosol detection frequencies were much lower than those observed by CALIOP. To improve upon the current ATL09 data products, a new ICESat-2 research data product has been developed providing de-noised daytime profiles, improved cloud and aerosol layer detection, feature subtyping, and layer optical depth. Denoising the daytime data is completed using a deep neural network model (Selmer et al., 2024; Gomes et al., 2025). Atmospheric layer detection and cloud-aerosol discrimination are accomplished utilizing a convolutional neural network (CNN) that has been shown to improve layer detection, including challenging multi-layer scenes (Yorks et al., 2021; Oladipo et al., 2024). Cloud phase and aerosol type are determined for detected layers using MERRA-2 reanalysis meteorological fields and aerosol optical depths (Nowottnick et al., 2022).

The GLOVE campaign, with its inclusion of the CPL instrument, provides a valuable dataset for validating the operational ATL09 and new ICESat-2 research data products (McGill et al., 2007; Yorks et al., 2011b; Hlavka et al., 2012; Yorks et al., 2016; Pauly et al., 2019; Palm et al., 2021). The fine resolution and high SNR CPL data provide as close to a "truth" lidar dataset as is possible, which is critical in evaluating the representation of tenuous cirrus cloud and aerosol features in the daytime ATLAS data. CPL total attenuated backscatter enables evaluation of the ICESat-2 calibration provided in the ATL09 data products. The linear depolarization measurements available with CPL facilitate more accurate feature subtyping than is possible with current ATLAS capabilities and will be used to evaluate the CNN-derived cloud-aerosol discrimination and model-assisted feature subtypes in the new research data products. Scenes of interest for

Table 1. Lidar specification for spaceborne EarthCARE and ICESat-2 compared to airborne CPL and Roscoe.

Parameter	ATLAS	ATLID	CPL	Roscoe
Wavelengths	532 nm	355 nm	355, 532, 1064 nm	355, 1064 nm
Depolarization	NA	355 nm	1064 nm	355, 1064 nm
Vert. Res.	30 m	103/500 m	30 m	30 m
Data Frame	14 km	40 km	18–20 km	40 km
Footprint	45 m/6 km	< 32 m	2 m	1 m
Pointing	3°	5°	Nadir*	Nadir*

* While CPL and Roscoe point nadir, the ER-2 flies with a nose-up pitch attitude of a few degrees. NA – not available.

Table 2. Radar specification at the surface for spaceborne CPR compared to airborne CRS.

Parameter	CPR	CRS
Frequency	94 GHz	94 GHz
Footprint	~ 750 m	~ 160 m
Vert. Res.	100/500 m	125 m
Sensitivity (@ 10 km)	-36 dBZ	-36 dBZ
Doppler Range	$\pm 10\ \mathrm{m\,s^{-1}}$	$\pm 14.2\ \mathrm{m\,s^{-1}}$
Pointing	Nadir	Nadir

ICESat-2 validation include different types of aerosols, cirrus clouds, cumulus and marine aerosol, and complex multilayer scenes.

2.2 EarthCARE Validation

The EarthCARE satellite (Wehr et al., 2023) is a joint ESA–JAXA mission carrying four remote sensing instruments. The Atmospheric Lidar (ATLID) is a HSRL that provides vertical profiles of aerosols and thin clouds at 355 nm with depolarization capabilities, as shown in Table 1 (Donovan et al., 2024). The Broad-Band Radiometer (BBR) measures reflected solar and emitted thermal radiances at the TOA using one SW and one LW channel with three fixed viewing directions. The Cloud Profiling Radar (CPR) is a Doppler cloud profiling radar (94 GHz) that observes vertical profiles of clouds and their vertical motion (Table 2). The Multi-Spectral Imager (MSI) provides wide-scene observations of clouds and aerosols using channels in the visible, near infrared, shortwave-infrared and thermal infrared (Table 3). The data from these instruments, both individually and combined, provide cloud, aerosol, precipitation, and radiation products to understand the interactions of clouds and aerosols with radiation.

EarthCARE single-instrument L2 products became available in December 2024 to the EarthCARE validation teams, before the public release of the consolidated data products in March 2025. EarthCARE aerosol, cloud, precipitation, composite and synergistic products and their main references are listed in Table 1 of Mason et al. (2024). These products can be classified in six groups: (1) ATLID retrievals of profiles of ice clouds (A-ICE) and aerosols (A-AER and A-EBD), (2) ATLID cloud top height and aerosol layer descriptor (A-LAY), (3) CPR retrievals of ice and liquid clouds, snow, and rain (C-CLD) and corrected Doppler measurements (C-CD), (4) MSI cloud mask (M-CM), retrievals of cloud optical properties (M-COP) and retrievals of aerosol properties (M-AOT), (5) a composited cloud, aerosol, and precipitation product (ACM-COM) and (6) a simultaneous and unified retrieval of cloud, aerosol, and precipitation (ACM-CAP). Note that the EarthCARE processing chain also includes an operational 3D radiative transfer product (ACM-RT) that provides computed profiles of atmospheric heating rates and TOA SW and LW fluxes. These fluxes are automatically compared with EarthCARE broad-band radiometer measurements, allowing for a radiative closure assessment of the retrieved cloud and aerosol properties.

There are many EarthCARE validation activities underway, including validation projects funded through ESA and JAXA. Scientists in the ESA ECVT collaborate with the mission's algorithm and instrument experts, as well as the leads for the validation projects. While there were as many as 59 EarthCARE validation segments flown in previous field campaigns (before GLOVE), few of these segments included combined airborne measurements from lidar, Doppler radar, and spectrometers operating at the EarthCARE frequencies. Furthermore, by the start of the GLOVE deployment, the atmospheric scenes that were the most sampled were marine clouds, with fewer observations of scenes such as cirrus and precipitating clouds. The active weather patterns in the GLOVE region (Western US) and timeframe (February 2025) provided ample opportunity to sample cirrus and precipitating clouds, and the inclusion of three similar remote sensors enables a validation dataset for EarthCARE multi-sensor combined data products. The validated operational EarthCARE L1 and L2a data products are being used for data gap-filling activities and data assimilation of EarthCARE products in the European Centre for Medium-Range Weather Forecasts (ECMWF) Numerical Weather Prediction (NWP) Model.

Table 3. Spectrometer specification for spaceborne MSI compared to airborne eMAS.

Parameter	MSI	eMAS
VIS Bands	0.67 µm	0.55, 0.66, 0.70 µm
NIR Bands	0.87 µm	0.83, 0.87, 0.91 µm
SWIR Bands	1.65, 2.21 µm	1.61, 1.66, 2.18, 2.23 µm
TIR Bands	8.8, 10.8, 12.0 µm	8.55, 10.2, 11.03, 12.02 µm
Swath Width/Symmetry	150 km/Asymmetric	37 km/Symmetric
Pixel Res.	500 m	50 m
Pointing	Nadir	Nadir

2.3 Targeted Scenes and Deliverables

The GLOVE Mission Scientists developed a list of targeted scenes (Table 4) starting with a set of meteorological conditions that present unique challenges for EarthCARE retrieval algorithms. This list, which was established by the EarthCARE Joint Mission Advisory Group (JMAG), was provided to the GLOVE team by the ESA ECVT and corroborated by the JAXA EarthCARE team over several pre-deployment telecons. Several scenes on this list, such as cirrus clouds and mixed aerosol types, also serve as good cases for testing the ICESat-2 current and new research data products. Two additional scenes were added to the ECVT list: (1) aerosols that are a single type over land or ocean, specifically to test ICESat-2 data products, and (2) upper troposphere-lower stratosphere (UTLS) aerosols that also provided an opportunity to quantify the zenith channel performance of one of the airborne lidars. This list was used to create the project scorecard and track progress in real time during the field campaign so the team could choose the scene of highest priority for a given flight.

GLOVE had five deliverables identified before the deployment, as specified below:

1. Collect 3–5 ICESat-2 underflight cases.
2. Collect 2–4 EarthCARE underflight cases.
3. Produce and publish CPL standard L1 and L2 data products for deliverables #1 and #2.
4. Produce and publish CRS and eMAS standard L1 data products for deliverable #2.
5. Collect 20 h of Roscoe data.

The team was able to achieve or exceed four of the five deliverables. We collected 7 ICESat-2 underflight cases, producing and publishing CPL data for all cases. We sampled 6 EarthCARE cases, producing and publishing CRS data for all cases and eMAS data for 3 cases. Unfortunately, we only collected 11.9 h of Roscoe lidar data, and the data quality was poor due to a laser alignment issue. More details about the GLOVE observations are provided in Sect. 3.

3 Observations

GLOVE was an efficient and affordable validation field campaign that utilized high heritage instruments, experienced team members (Fig. 2), local aircraft resources, and several funding sources. The CPL, CRS, and eMAS have flown together, in some combination, in multiple field campaigns, such as the Investigation of Microphysics and Precipitation for Atlantic Coast-Threatening Snowstorms (IMPACTS), Radar Definition Experiment (RADEX), Studies of Emissions and Atmospheric Composition, Clouds, and Climate Coupling by Regional Surveys (SEAC4RS), and Tropical Composition Cloud and Climate Coupling (TC4). GLOVE mission scientists and forecasters leveraged their experience from serving similar roles during IMPACTS, Convective Processes Experiment – Cabo Verde (CPEX-CV), Westcoast & Heartland Hyperspectral Microwave Sensor Intensive Experiment (WH2yMSIE), and Arctic Radiation-Cloud-Aerosol-Surface Interaction Experiment (ARCSIX). Using NASA Armstrong Flight Research Center (AFRC) as the deployment location reduced mission costs and improved communication but did come with operational constraints. More details about the GLOVE instruments, operations, and performance are provided below.

3.1 Instruments and Data Products

3.1.1 CPL

The CPL utilizes a high repetition rate, low pulse energy transmitter and photon-counting detectors (McGill et al., 2002). The CPL fundamentally measures the total (particulate plus Rayleigh) attenuated backscatter as a function of altitude at three wavelengths (355, 532, and 1064 nm, with depolarization measurement at 1064 nm). It is designed to withstand the thermal and vibration environment of the ER-2 aircraft without misalignment and operation is fully autonomous. A list of the primary instrument parameters is given in Table 1. Figure 1 shows the CPL instrument housed in the forward section of the ER-2 left wing superpod for GLOVE. The CPL was built during 1999–2000 and was immediately deployed to South Africa for the Southern African Regional Science Initiative (SAFARI-2000) field campaign

Table 4. Targeted number of scenes for EarthCARE and ICESat-2 validation. GLOVE Objectives: I = ICEsat-2 validation, E = EarthCARE validation, R = Roscoe data collection.

Scenes of Interest	GLOVE Obj.	ICESat-2 Obs	EarthCARE Obs	NPP Obs
Aerosols (mixed types over land)	I, E, R	1		
Aerosols (single type, land or ocean)	I, E, R	1		
Cumulus and marine aerosol	I, E, R	1	2	1
Marine stratocumulus	I, E, R		1	1
Largescale rain	E			
Snow, including snow above melting layer	E		2	
Altocumulus and cold-air outbreaks	E			
Cirrus	I, E, R	6	4	2
Complex multilayer scenes	I, E, R	3	5	
Deep convection	E			
UTLS Aerosol Plumes	I, E, R			

Figure 2. A portion of the GLOVE team with the NASA ER-2 at the NASA Armstrong Flight Research Center in Edwards, California. Credit: NASA/Steve Freeman.

(McGill et al., 2003; Schmid et al., 2003) Since then, the CPL has participated in nearly 30 field campaigns, accumulating several thousand hours of data. Higher order data products derived from the attenuated backscatter include cloud top heights, cloud phase, aerosol layer heights, feature optical depth, and extinction coefficient vertical profiles (Yorks et al., 2011a; Hlavka et al., 2012).

The CPL high SNR, fine resolution (both vertical and horizontal), and minimal multiple scattering enable accurate feature detection even at low optical depths, making CPL a comprehensive validation tool for spaceborne lidar systems (e.g., McGill et al., 2007; Yorks et al., 2011b; Hlavka et al., 2012; Yorks et al., 2016). The quality of data products from CPL is a function of signal-to-noise ratio (SNR), multiple scattering, and calibration uncertainty. Due to its narrow field of

view (100 microradians) and altitude of the airborne platform (∼ 20 km), CPL achieves reduced multiple scattering effects (∼ 5 %) and high SNR at 532 and 1064 nm (McGill et al., 2002). Standard calibration procedures include normalization to the atmospheric molecular profile within an altitude range of 15–18 km. Therefore, the 532 and 1064 nm attenuated backscatter uncertainties are 2 %–6 % and 4 %–9 %, respectively (McGill et al., 2007; Pauly et al., 2019). The depolarization ratio is calibrated using the relative gain between the perpendicular and parallel channels (polarization gain ratio) with crosstalk between the channels of ∼ 3 %. This results in a depolarization uncertainty of 5 %–10% (Liu et al., 2004). The well-calibrated, high SNR CPL backscatter data at 532 nm makes it a valuable calibration tool for ICESat-2 Level 1 atmospheric data products, which have calibration uncertainties of < 10 % at night and < 20 % during daytime (Palm et al., 2021). Implications of CPL lidar ratio uncertainties propagate into higher-order estimates of cloud and aerosol geophysical variables, leading to extinction coefficient uncertainties at 532 and 1064 nm of 25 %–80 % (Yorks et al., 2011a; Hlavka et al., 2012). Furthermore, lower SNR at 355 nm due to lower laser power at that wavelength limits the use of CPL for validating EarthCARE aerosol extinction retrievals, which have a required accuracy of 15 % (Wehr, 2006). However, CPL cloud top and base height uncertainties on the order of less than 60 m make it ideally suited for validation of EarthCARE (300 m requirement) and ICESat-2 vertical cloud feature mask products (Vaughan et al., 2009; Yorks et al., 2011b, 2021).

3.1.2 Roscoe

Roscoe is a backscatter lidar with heritage from the long-standing CPL. Roscoe is designed to operate simultaneously at 1064 and 355 nm, with depolarization measurement at both wavelengths. To avoid increasing challenges with airborne laser safety, Roscoe is intentionally designed without visible wavelengths, enabling unrestricted operation at night over areas (e.g., airports, military zones) typically off-limits for instruments operating in the visible. Roscoe is designed to look both nadir and zenith from the airborne platform to permit studies of both tropospheric and stratospheric aerosols. Like the CPL, Roscoe utilizes a high repetition rate, low pulse energy laser and photon-counting detection. Primary instrument parameters are listed in Table 1. The Roscoe instrument employs a solid-state, diode-pumped, conductively cooled laser operating at 10 kHz repetition rate. The laser simultaneously transmits 1064 and 355 nm light, switching every other pulse between the up and down direction. The receiver uses solid state photon-counting detectors to measure the backscattered light at both wavelengths in both directions. The Roscoe lidar was housed in the forward section of an ER-2 right wing superpod for GLOVE (Fig. 1). A specific superpod has been modified to have an up-looking window. Similar to CPL, the fundamental Roscoe data product is total attenuated backscatter as a function of altitude at each wavelength. Higher order data products are identical to CPL. The vertical resolution of the Roscoe measurements is 30 m, and horizontal resolution can vary but is typically 200 m. For tropospheric measurements the purpose of Roscoe is like that of the CPL: to provide measurements of cirrus, subvisual cirrus, and aerosols with high temporal and spatial resolution. For stratospheric measurements the depolarization measurement capability permits determination of smoke layers and stratospheric sulfate layer/ash layers.

Initial Roscoe engineering test flights were conducted on the ER-2 in October 2019. When the WB-57 was modified to carry the ER-2 superpods, Roscoe was operated from the WB-57 as part of the Asian Summer Monsoon Chemical and Climate Impact Project (ACCLIP) and Stratospheric Aerosol processes, Budget and Radiative Effects (SABRE) field campaigns. During the ACCLIP field campaign, the Roscoe laser optics became misaligned, and the laser energy showed a strong temperature dependence, reducing data quality and SNR during some of the WB-57 flights. Engineers at NASA GSFC replaced the laser optical bench and realigned the laser after the ACCLIP mission. Roscoe's inclusion in GLOVE was to test the performance of the Roscoe lidar and not as a source of ICESat-2 and EarthCARE validation. Unfortunately, the ER-2 experienced severe turbulence in the first GLOVE flight over southeastern California, causing a small screw to an optic in the Roscoe laser to become dislodged and wedged on another optic, blocking the transmitter path and preventing the laser light from exiting the instrument. Roscoe flew the first two GLOVE flights but collected no science quality data and was then removed for the rest of the deployment. Once back at GSFC, the optic was fixed and ground tests are demonstrating high quality Roscoe data once again, with plans to fly on the ER-2 sometime in 2026.

3.1.3 CRS

The CRS is a W-band (94 GHz) solid-state Doppler radar (Walker McLinden et al., 2021). CRS operates from the aft section of either ER-2 superpod in a near-nadir configuration, providing reflectivity, Doppler velocity, and Doppler velocity spectrum width estimates. Figure 1 shows the location of the CRS system installed in the ER-2 for GLOVE. Originally developed in the 1990's as a high-power extended-interaction klystron (EIK)-based radar (Li et al., 2004), CRS has been comprehensively updated two times. In 2014 the EIK transmitter was removed in favor of a 30 W solid-state power amplifier (SSPA). The system was fully upgraded in 2022 including new mechanical/structural systems, electronics, and a 50 W SSPA. Throughout its history CRS has flown in numerous field campaigns. GLOVE is the fourth field campaign in which CRS has flown in its most-recent configuration.

The CRS specifications are provided in Table 2 along with the EarthCARE CPR specifications. CRS has sensitivity better than −30 dBZe, with approximately 115 m vertical reso-

lution and 180 m horizontal resolution. The data are sampled every 26.25 m vertically and 50 m horizontally. The pulse compression sidelobes are approximately −70 dB. The system uses a staggered pulse-repetition frequency (PRF) to provide an unambiguous Doppler velocity of 14.25 m s^{-1}. Level 1B data products from CRS include corrections to the Doppler velocity from aircraft motions as well as the effects of horizontal winds due to slight off-Nadir pointing. The residual error in vertical Doppler velocity estimates is less than 0.5 m s^{-1}. Reflectivity is calibrated using the ocean surface backscatter during roll maneuvers (Li et al., 2005; Walker McLinden et al., 2021), with an estimated calibration uncertainty of 1 dB. This performance, while not alone able to fully validate EarthCARE CPR's goal of 1.0 m s^{-1} Doppler accuracy (Wehr, 2006), is sufficient to bound its uncertainty and evaluate the effects of limited resolution and non-uniform beam filling (NUBF). Current CRS Level 1 data do not include a Doppler velocity spectrum width product, however both spectrum width and limited Doppler spectra are possible future products that may be added. The high spatial resolution of the airborne CRS reflectivity and Doppler velocities also provide an avenue to evaluate spectrum width from CPR.

3.1.4 eMAS

The Enhanced MODIS Airborne Simulator (eMAS) was originally developed in the early 1990s for deployment on the high-altitude ER-2 aircraft (King et al., 1996) to support the development and validation of atmosphere algorithms for the soon-to-be launched Moderate-resolution Imaging Spectroradiometer (MODIS). eMAS consists of four spectrometers – two shortwave (SW) grating spectrometers, one longwave infrared (LWIR) grating spectrometer, and one mid-wave IR (MWIR) filter radiometer – coupled to a single scan mirror and telescope. In 2009, a replacement module for the coupled MW/LWIR spectrometers was designed and fabricated that provided thermal isolation (compared to the original design) and mechanical cooling (previously liquid nitrogen dewars) enabling long-duration flight operations. The eMAS scan head scans through nadir in a plane perpendicular to the velocity vector of the aircraft (cross track), with the maximum scan angle extending roughly 43° on either side of nadir, or roughly 86° full swath. A total of 716 Earth-viewing pixels, each having a 2.5 mrad (0.14°) instantaneous field of view, are acquired per scan at a scan rate of 6.25 Hz. Thus, from a nominal ER-2 altitude of 20 km, eMAS observes a 37 km wide ground swath centered on the aircraft ground track with a 50 m pixel size (Table 3). eMAS observes reflected solar and emitted thermal spectral radiation in 38 narrowbands having spectral coverage similar to MODIS (visible through the 14 µm CO_2 bands). Since its development, the imager has flown in numerous field campaigns throughout the world, observing Arctic stratus over sea ice in polar regions (Platnick et al., 2001; King et al., 2004), marine stratocumulus clouds off the coasts of California and Namibia (Platnick et al., 2000; King et al., 2003; Meyer et al., 2025a), biomass fires (King et al., 1998, 2003; Shi et al., 2024), and tropical/subtropical convective systems over the U.S. and surrounding waters (Chiriaco et al., 2007; Meyer et al., 2016) and Central America (Jensen et al., 2009; King et al., 2010), among many others.

eMAS has served as a critical validation tool for four decades for spaceborne imagers such as MODIS, the Visible Infrared Imaging Radiometer Suite (VIIRS), and the Advanced Baseline Imager (ABI) due to its fine spatial resolution and high accuracy. Radiometric assessments show eMAS at-sensor radiances agree with other airborne and space borne imagers, and calculations based on ground vicarious calibration sites, to within 5 % in the shortwave (e.g., Bruegge et al., 2021), consistent with results from similar airborne radiometric assessments (e.g., McCorkel et al., 2016). Radiometric comparisons with airborne IR interferometer sounders (e.g., Scanning High-Resolution Interferometer Sounder) show eMAS IR brightness temperatures (BTs) agree to within 1 K for most LW channels, meeting or exceeding the 1 K radiometric accuracy requirement of the EarthCARE MSI LW channels. Regardless of absolute radiometric accuracy, however, the high spatial resolution eMAS observations also provide key sub-pixel context subpixel context in spectrally relevant channels for assessing coincident EarthCARE MSI observations and retrievals.

3.2 Operations

For a given GLOVE flight, a 30 min satellite validation segment is identified and targeted, as shown in Fig. 3. EarthCARE satellite tracks were obtained through collaboration with the ECVT coordinators. The EarthCARE mission analysis engineer provided the GLOVE team with the most up-to-date EarthCARE track KML files for the western US region (domain of 50 to 20° N; 135 to 105° W) that included predicted changes due to any orbital manoeuvres, which are typically not available in predictions based on TLE. The GLOVE team identified validation opportunities 2–3 d in advance, providing the orbit number of possible underflight targets to the ECVT. These tentative opportunities were then communicated to the EarthCARE instrument and flight planning engineers, so they could ensure nominal science operations during these orbits or warn the GLOVE and ECVT teams in the event of unavoidable conflicting activities. This information was also used to generate EarthCARE quicklooks after the GLOVE underflights. The ICESat-2 Instrument Support Facility reserved a geographical domain for which the satellite pointed over a series of pre-defined reference ground tracks (RGTs) during the GLOVE deployment to ensure precise orbit tracks for validation purposes with the ER-2 aircraft. The specific RGT number corresponding to an overpass of interest was obtained from a time-specific orbit dataset that contained nominal timestamps for each of

the 1387 RGTs. Once the ICESat-2 and EarthCARE satellite tracks of interest were identified, the GLOVE team would choose the best segment based on weather and operational constraints.

Weather forecasting efforts during GLOVE involved daily morning briefings focused on meteorological, aerosol, cloud, and precipitation products over the Eastern Pacific Ocean, Intermountain West and West Coast of the United States. Meteorological products of interest included mean sea level pressure and low-level wind 3–5 d forecasts from the Global Forecast System (GFS) and ECMWF models. Aerosol products included optical thickness from dust, organic carbon, black carbon, and all aerosols from the NASA Goddard Earth Observing System Model, Version 5 (GEOS-5). Cloud fraction and precipitation rate products from the North American Mesoscale (NAM) forecast system were used to estimate the likelihood of high and low cloud cover along the satellite tracks. GLOVE forecasters, in collaboration with local forecasters at Edwards AFB, were also tasked to provide runway conditions pertaining to the ER-2 aircraft limitations, such as crosswind (sustained and gusts), ceiling heights, and precipitation probability. Finally, forecasters aided dynamic adjustments to the ER-2 track during flight with near real-time updates of cloud and precipitation trends as necessary. Real-time monitoring by mission scientists and forecasters was done using NASA's Mission Tools Suite (MTS; https://mts2.nasa.gov, last access: 27 May 2026).

The GLOVE mission scientists used the satellite tracks and weather forecasts, detailed above, to construct each individual flight plan. In cases when there were scenes of interest along both satellite tracks but only one track could be flown, the GLOVE scorecard was referenced to prioritize scenes under a satellite that had not been sampled earlier in the project. In many flights (4 of 8), the satellite tracks were separated by less than 400 km and 50 to 100 min apart, enabling flights with both ICESat-2 and EarthCARE underflight segments over scenes of interest. Once the underflight segment(s) were identified, the latitude, longitude, and time of the segment(s) were given to the ER-2 navigator, who then created a tentative flight plan 1–2 d in advance of the flight. Underflight segments were adjusted as necessary to avoid restricted airspace and changing weather forecasts. Secondary science objectives, such as Suomi National Polar-orbiting Partnership (NPP) underflights, eMAS calibration legs over Railroad Valley (Nevada), CRS calibration manoeuvres over ocean, or additional scenes of interest, were added to the flight plans if feasible.

GLOVE operated during February 2025 out of NASA AFRC, within Edward AFB in southern California, which is the operations base for the NASA ER-2. Operating at the ER-2 base offered GLOVE several benefits:

- Access to land and ocean, as it is located about 150 km north of Los Angeles and east of the Pacific Ocean
- Abundance of atmospheric features within the ER-2 range during the winter months, which tends to be an active period for atmospheric river systems in the region
- Reduced costs, as the project did not have to fund ER-2 crew and staff travel
- Improved communications given the GLOVE scientists and ER-2 staff were all centrally located

However, there were some operational constraints at Edwards AFB, which included:

- A limited daily flight window between 06:00 and 22:00 LT
- Airfield closures over the weekends and national holidays
- Airfield closures due to Air Force activities
- Proximity to restricted airspaces, both off the coast and over parts of California and Nevada

GLOVE was able to meet or exceed all its pre-deployment deliverables, so the advantages outweighed the constraints for the scenes and validation objectives of GLOVE. The daytime flight window prevented nighttime data collection, which would have been useful cases to assess nighttime ICESat-2 and ATLID data products under optimal performance. However, daytime scenes are more valuable for ICESat-2 and EarthCARE validation. Visible spectrometer data products from both eMAS and MSI are only available during day, and spaceborne lidar data products have larger uncertainties during daytime than night due to solar background noise (Selmer et al., 2024).

3.3 Flight Tracks and Summary

GLOVE accumulated 8 flights between 3–20 February 2025, for a total of roughly 40 flight hours. Flight tracks are plotted in Fig. 4 and details of each flight are provided in Table 5. Takeoff times were between 18:00 and 20:00 UTC, and flight durations ranged from 4 to 6 h. A total of 7 ICESat-2 validation segments, 6 EarthCARE validation segments, and 3 NPP underflights were performed. As previously discussed, Roscoe only flew on the first 2 flights, but no science quality data was collected due to the laser alignment issues. The data system for eMAS experienced an initialization failure during the campaign's combined system test (CST) on 31 January 2025. After iterative testing, the issue was isolated to the main computer board and the board was replaced. eMAS couldn't fly until it was reintegrated and successfully completed a CST, per aircraft operational standards, which was performed before the 12 February flight. eMAS participated in the last 4 flights of the project, providing science quality data for 3 EarthCARE and 3 NPP underflight segments. Both CPL and CRS performed very well during all eight GLOVE

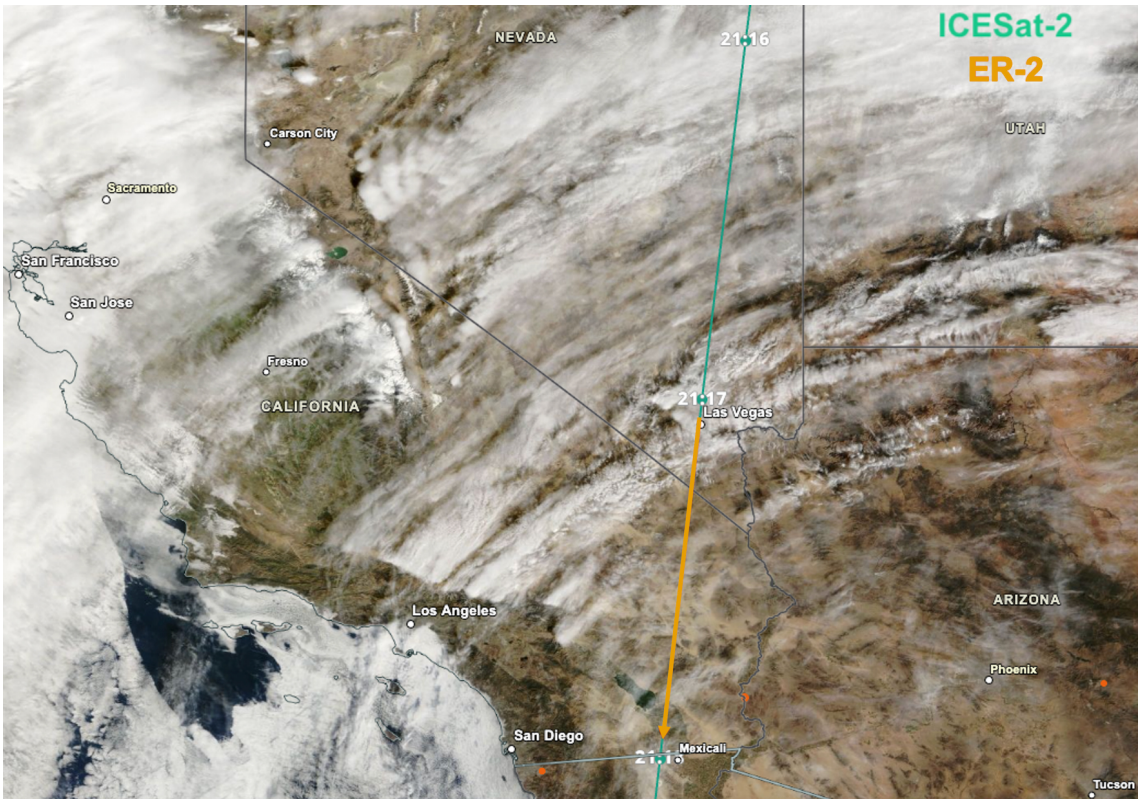

Figure 3. An example of the targeted satellite track (green, ICESat-2) and the roughly 30 min long ER-2 underflight segment (orange) on 3 February 2025. The satellite and aircraft tracks are overlaid on the True Color Corrected Reflectance from MODIS on the Terra satellite, which shows optically thin cirrus clouds over southern California.

flights, including all 7 ICESat-2 underflights and all 6 EarthCARE underflights.

GLOVE collected data of seven different scenes of interest, as shown in Tables 4 and 5. Many flights over land targeted cloud scenes, especially cirrus clouds, ahead of approaching atmospheric river systems. Small aerosol plumes (dust, smoke, or a mixture) were also observed over land, but no widespread aerosol events occurred during the GLOVE timeframe. Flights over ocean targeted stratocumulus clouds, marine aerosols, and multi-layer scenes. Several targeted scenes, such as UTLS aerosols, deep convection, and altocumulus/cloud-air outbreaks, were not observed in the GLOVE observational domain during February of 2025. Other scenes such as largescale rain or polluted continental aerosol types were observed but not along satellite tracks during operational sampling times (i.e., daytime during the weekdays), occurred in restricted airspace, or in the case of widespread rain grounded the ER-2 for the day when it occurred at AFRC.

GLOVE observed aerosols, cirrus clouds, cumulus and marine aerosols, and complex multi-layer scenes during the seven ICESat-2 underflight segments (Table 4). Aerosols over land, possibly dust or smoke or a mixture, were observed on 3 and 7 February. These aerosol plumes were

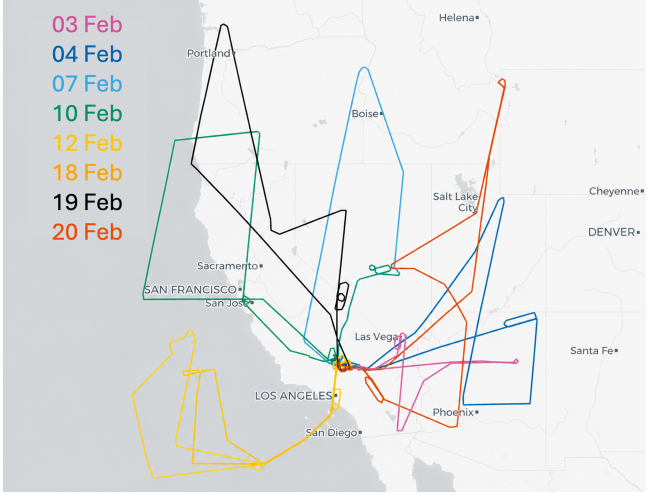

Figure 4. Flight tracks for the GLOVE field campaign. Eight flights were conducted from 3–20 February 2025 over California, Nevada, Arizona, Oregon, Utah, Idaho, and the coastal Pacific Ocean from the Armstrong Flight Research Center in Edwards, California.

Table 5. Daily description of GLOVE flights. Eight flights, with a total of 40 flight hours, were carried out between 3 to 20 February 2025 for 13 total validation segments.

Flight Date	Takeoff (UTC)	Duration (hours)	Scenes of interest observed	Instrument status	Satellites Overpasses	Notes
3 Feb	19:39	4.3	Cirrus, aerosols, complex multilayer scenes	CPL and CRS functioning normal, no eMAS, Roscoe data quality was poor	ICESat-2 (21:17)	Cirrus and aerosols, possibly from small fires, were observed in southern CA along satellite track (Fig. 5), as well as from a small smoke plume near Flagstaff.
4 Feb	18:57	5.3	Cirrus, cumulus	CPL and CRS functioning normal, no eMAS, Roscoe data quality was poor	ICESat-2 (20:52), EarthCARE (21:47)	Cirrus along both the ICESat-2 and EarthCARE tracks. Continental clear air and small cumulus clouds were observed below the cirrus (Fig. 8), but some optically thicker aerosols were sampled before the satellite lines.
7 Feb	19:45	5.2	Aerosols (mixed type over land), complex multilayer scenes	CPL and CRS functioning normal, no eMAS and Roscoe	ICESat-2 (21:08), EarthCARE (22:15)	Clouds of varying altitudes and an aerosol plume along the ICESat-2 track. Persistent clouds below 7 km along the EarthCARE track.
10 Feb	20:03	4.7	Cirrus, aerosols, cumulus and marine aerosols, complex multilayer scenes	CPL and CRS functioning normal, no eMAS and Roscoe	ICESat-2 (21:25), EarthCARE (22:46)	Cirrus present at ICESat-2 rendezvous point. Cirrus, possibly aerosol layer aloft, and marine aerosols present at EarthCARE rendezvous point
12 Feb	19:27	5.3	Marine stratocumulus, cumulus and marine aerosols, complex multilayer scenes	CPL, CRS, and eMAS functioning normal, no Roscoe	NPP (21:29), EarthCARE (22:36)	Extensive marine stratus for NPP leg; small shallow rain features at time of EarthCARE coincidence (Fig. 7).
18 Feb	19:01	4.3	Cirrus, aerosols, cumulus and marine aerosols, complex multilayer scenes	CPL, CRS, and eMAS functioning normal, no Roscoe	ICESat-2 (21:09), NPP (21:18)	Lots of high-altitude (12–15 km) cirrus, occasional marine aerosol. 2 calibration maneuvers for CRS.
19 Feb	19:31	5.1	Cirrus, complex multilayer scenes	CPL, CRS, and eMAS functioning normal, no Roscoe	ICESat-2 (20:43), NPP (21:22–22:23), EarthCARE (22:40)	Many cirrus clouds were sampled. NPP line was parallel to the actual NPP track but offset between 20–80 min along the line from the time of satellite overpass.
20 Feb	18:47	5.7	Cirrus, aerosols, snow, complex multilayer scenes	CPL and CRS functioning normal, eMAS occasional degredation in eMAS 11.03 µm channel, no Roscoe	ICESat-2 (20:18), EarthCARE (21:49)	Low dust concentrations (CPL) along ICESat-2 line. Impressive snow along south half of EarthCARE overpass (Fig. 6). Railroad Valley calibration leg (21:06 UTC) may have had small cloud over site.

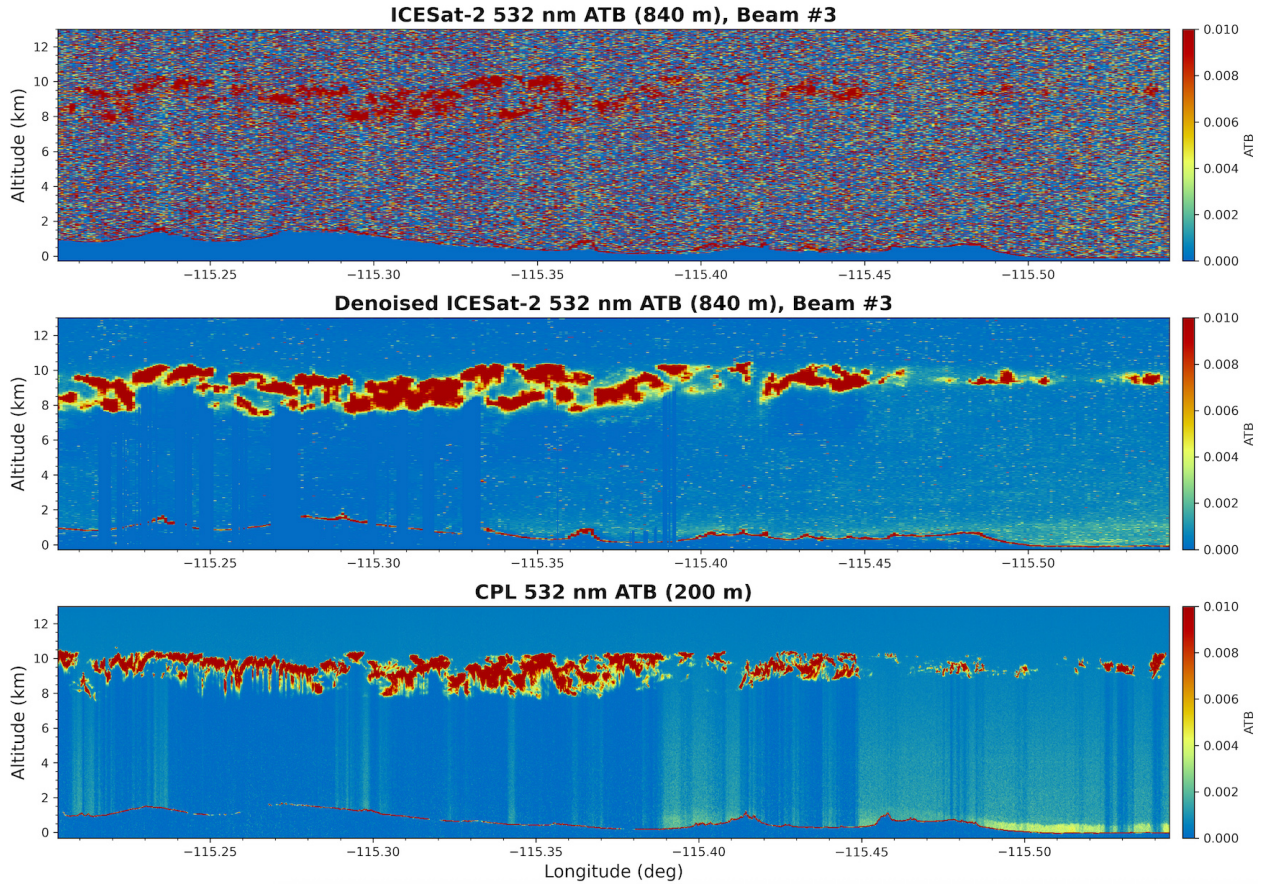

Figure 5. The 532 nm attenuated total backscatter (ATB, km^{-1} sr^{-1}) curtain plots for the standard ICESat-2 ATL09 data product (top panel) and denoised research ICESat-2 data product (middle panel) at 1.12 km horizontal resolution, as well as the CPL 532 nm ATB (bottom panel) at 200 m horizontal resolution, show cirrus clouds between 8 and 11 km altitude as the ER-2 flew from southern Nevada to southern CA on 3 February 2025 (track in pink, Fig. 4).

small scale and will likely be difficult for ICESat-2 to detect given they were observed during daytime hours. The flight on 18 February was out over the Pacific Ocean, where marine aerosols and cumulus clouds were present. Optically thin cirrus clouds, observed during six validation segments (3, 4, 10, 18, 19, 20 February 2025), provide a robust way to test the denoising and layer detection algorithms for the new ICESat-2 research atmospheric data product. Additionally, lower-level clouds or aerosols were present below these cirrus clouds on 3, 18, and 19 February. One example from 3 February 2025 is shown in Fig. 5 as the ER-2 flew from southern Nevada to southern CA. The 532 nm attenuated total backscatter curtain plot from CPL (bottom panel) very clearly shows a cirrus cloud layer between 8 and 11 km altitude, as well as aerosols near the surface. Only the optically thickest parts of the clouds are visible in the operational ICESat-2 ATL09 data product (top panel), whereas the denoised (Gomes et al., 2025) research ICESat-2 data product (middle panel) shows more of the cirrus cloud layer but doesn't detect the aerosols near the surface. More quantitative comparisons of these ICESat-2 data products to the CPL data will be analysed in future publications.

GLOVE sampled six EarthCARE underflight segments, observing snow, cirrus clouds, stratocumulus, cumulus and marine aerosols, and complex multi-layer scenes (Table 4). The cases on 7 and 20 February captured clouds with frozen precipitation. One example of these regions of large precipitating hydrometeors, which are critical for validating the CPR Doppler velocity measurements, was sampled as the ER-2 flew over northern Utah on 20 February 2025 and is shown in Fig. 6. The 94 GHz reflectivity for CRS (top left) and CPR (bottom left) show good agreement despite the coarser resolution of CPR. The CPR Doppler velocity (bottom right) is noisier than the CRS Doppler velocity (top right) but is in good agreement otherwise. Flights on 10 and 12 February over the Pacific Ocean sampled stratocumulus clouds and scenes with mixed marine aerosols and cumulus clouds. Figure 7 shows False Color RGBs (0.67–1.6–2.1 µm) from MSI (left) and eMAS (right) of marine stratocumulus clouds on 12 February 2025. There is good agreement in

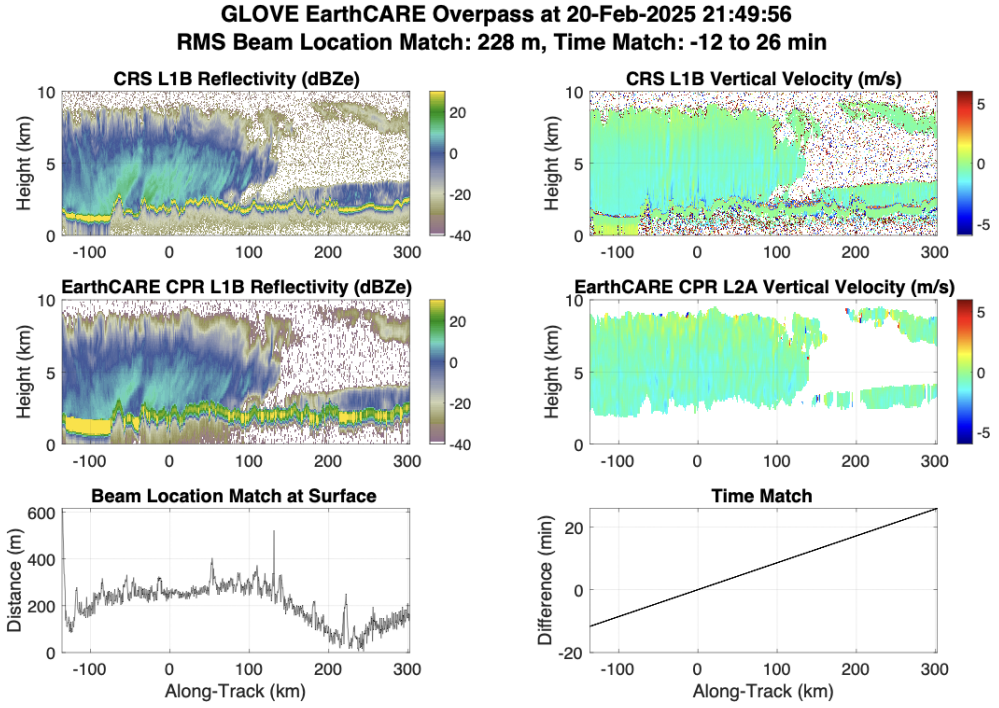

Figure 6. The 94 GHz reflectivity (left) and Doppler velocity (right) for CRS (top panels) and EarthCARE CPR BA baseline (middle panels) that show large and precipitating hydrometeors as the ER-2 flew over northern Utah on 20 February 2025 (track in red, Fig. 4). The bottom panels show the time match between the aircraft and EarthCARE satellite.

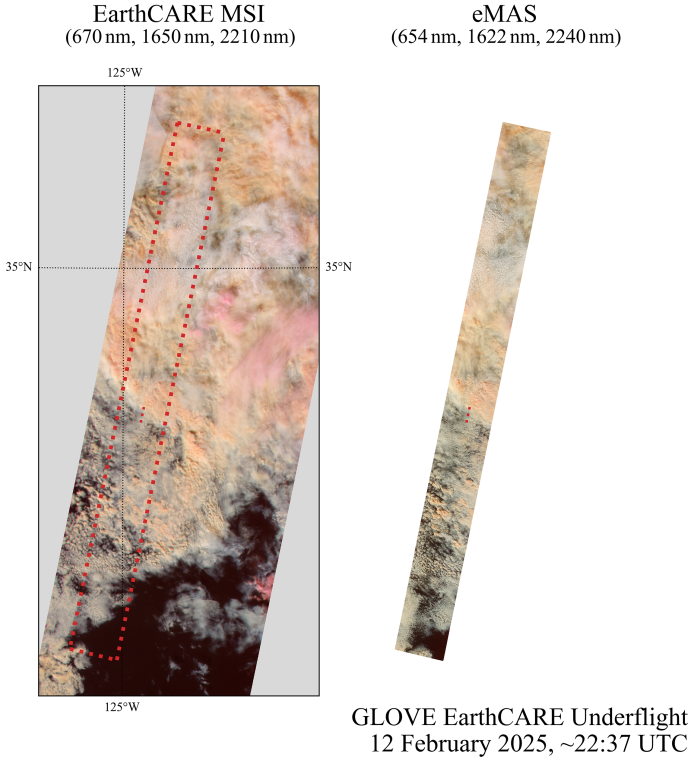

Figure 7. Merged images of 3 bands in the visible and short-wave infrared from the EarthCARE MSI instrument BA baseline (bands 670, 1650, and 2210 nm) and the eMAS instrument (bands 654, 1622, and 2240 nm) showing marine stratocumulus and cumulus clouds off the coast of California on 12 February 2025 at around 22:37 UTC (track in dark yellow, Fig. 4).

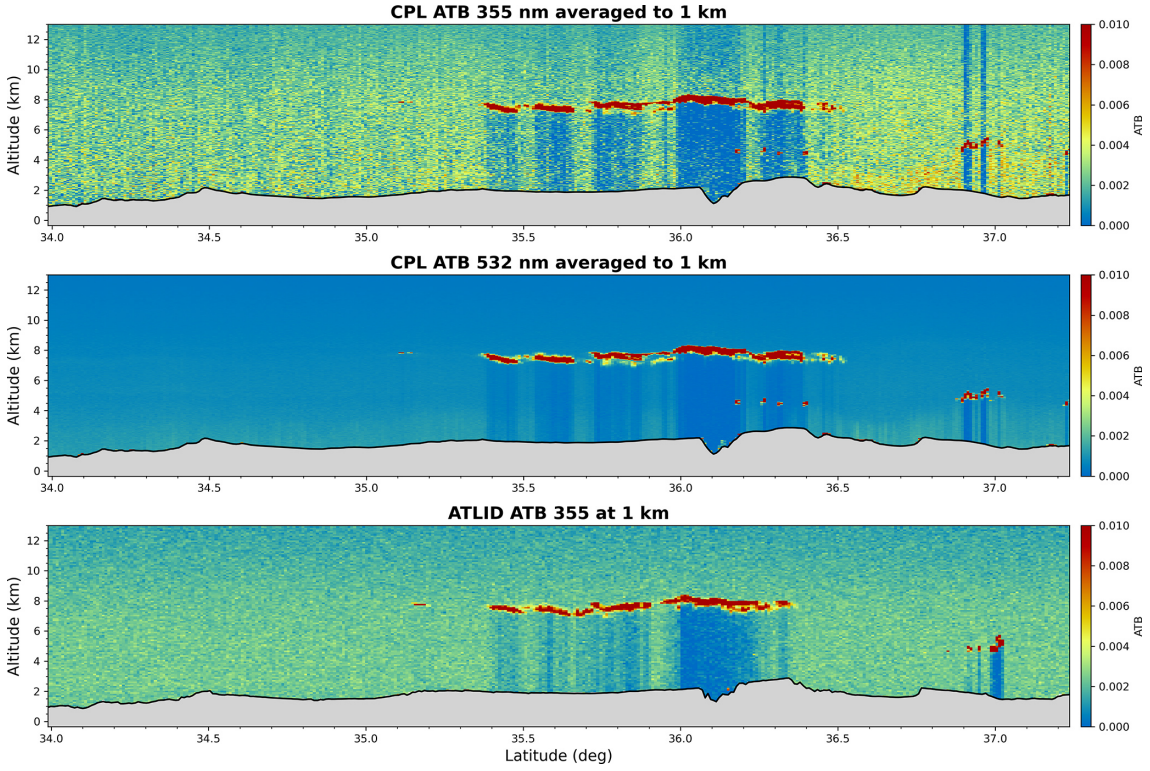

Figure 8. Curtain plots of attenuated total (Mie plus Rayleigh) backscatter (ATB, $km^{-1}\,sr^{-1}$) horizontally averaged to 1 km for CPL at 355 nm **(a)**, CPL at 532 nm **(b)**, and ATLID (BA baseline) aboard the EarthCARE satellite at 355 nm **(c)** show thin cirrus clouds between 7 and 8 km altitude as the ER-2 flew from northern Utah to southern Arizona on 4 February 2025 (track in dark blue, Fig. 4).

the cloud structure observed from both instruments, with the clouds becoming more broken in the southern half of the underflight segment. Cirrus clouds were observed during four validation segments (4, 10, 19, 20 February 2025), many with lower-level clouds below. Figure 8 shows the 355 nm (panel a) and 532 nm (panel b) attenuated total backscatter from CPL and the 355 nm backscatter coefficient from ATLID (panel c) for the EarthCARE validation segment on 4 February 2025. There is good agreement between ATLID and CPL cloud layer heights, as a geometrically thin cirrus cloud is observed between 7–8 km from 35.3 to 36.3 latitude in both the CPL and ATLID data. All the EarthCARE data used in these case studies are from the BA processing baseline. The EarthCARE and GLOVE teams plan collaboration on more detailed future analysis of these datasets.

4 Data availability

GLOVE is committed to providing freely accessible data to the community, especially ICESat-2 and EarthCARE data users. Browse images for the instruments are available at the individual instrument websites, are detailed below.

- CPL: https://cpl.gsfc.nasa.gov/ (last access: 27 May 2026)
- CRS: https://har.gsfc.nasa.gov/ (last access: 27 May 2026)
- eMAS: https://asapdata.arc.nasa.gov/emas/index.html (last access: 27 May 2026)

The primary repository for GLOVE data is Zenodo and the Level-1 and Atmosphere Archive and Distribution System (LAADS) DAAC, located at GSFC. Data for the three instruments can be downloaded at the website links below:

- CPL: https://doi.org/10.5281/zenodo.16807221 (Yorks et al., 2025)
- CRS: https://doi.org/10.5281/zenodo.17179580 (Walker McLinden et al., 2025)
- eMAS: https://doi.org/10.5067/GLOVE/EMAS/EMASL1B.002 (Meyer et al., 2025b).

The EarthCARE L1 and L2 data used in this paper are provided here: https://earth.esa.int/eogateway/missions/earthcare/data (last access: 27 May 2026; https://doi.org/10.57780/eca-e25465f, https://doi.org/10.57780/eca-7d84adf, https://doi.org/10.57780/eca-176429f, European Space Agency, 2025a, b, c), while the ICESat-2 data products can be found here: https://doi.org/10.5067/ATLAS/ATL09.001 (Palm et al, 2019).

5 Code availability

A GitHub repository that provides code for reading CPL and CRS data, as well as create plots (Finlon et al., 2025), can be found here: https://doi.org/10.5281/zenodo.15310597.

6 Conclusions

The GLOVE field campaign took place during February 2025 out of Edwards Air Force Base in California. The primary objectives of GLOVE were to validate ICESat-2 atmospheric data products, as well as EarthCARE lidar, radar, and spectrometer data products. GLOVE utilized the high-altitude NASA ER-2 aircraft, occupied with high heritage instruments CPL (lidar), CRS (Doppler radar), and eMAS (spectrometer) that provide similar capabilities to the instruments on the ICESat-2 and EarthCARE satellites. The Roscoe lidar also flew on the first two GLOVE flights, but an issue with the laser optical alignment prevented it from collecting science quality data and participating in the rest of the flights. GLOVE operations were efficient, as the project collected seven ICESat-2 and six EarthCARE underflight segments in just eight total flights (40 flight hours). Using NASA AFRC as the deployment location made the project more affordable and improved communication but did come with operational constraints such as limited flight possibilities due to airfield closures. GLOVE also prioritized training the next generation of airborne scientists, as it provided five early career scientists the chance to plan their first ever aircraft flights as mission scientists and offered four students participation in forecasting, instrument integration, and data processing efforts. With potential NASA budget constraints in the future, GLOVE provides a blueprint to performing affordable and efficient airborne projects for satellite validation.

The data collected during GLOVE, spanning seven different cloud and aerosol scenes over 13 satellite underflight segments, will be critical for validating EarthCARE and ICESat-2 atmospheric products. Optically thin features, such as cirrus clouds and small-scale aerosol layers, and complex scenes sampled during ICESat-2 underflights provide an opportunity to test the ability of the operational ATL09 and new research atmospheric data products to detect these layers during daytime hours. Quantifying detection and SNR improvements between the new research atmospheric data products and the operational ATL09 products enables users to appropriately use these data products for different applications and make more informed interpretations of the ICESat-2 data. The snow, cirrus clouds, stratocumulus, and complex multi-layer scenes will also provide a robust dataset to understand the limitations, accuracies, and reliability of the EarthCARE data. The CPR Doppler velocity measurements represent the first ever such measurements from space, and the GLOVE CRS data, especially of precipitating (snow) clouds, will be essential for quantifying the range of potential errors and uncertainties associated with these Doppler velocity measurements. Additionally, GLOVE is one of two mature airborne campaigns for EarthCARE validation (as of April 2025) that included lidar, radar, and spectrometer data, making it a unique opportunity to validate EarthCARE synergistic algorithms and data products.

Appendix A: Acronyms and units

Acronym	Definition
ABI	Advanced Baseline Imager
ACCLIP	Asian Summer Monsoon Chemical and Climate Impact Project
ARCSIX	Arctic Radiation-Cloud-Aerosol-Surface Interaction Experiment
ATLAS	Advanced Topographic Laser Altimeter System
ATL09	ICESat-2 atmospheric data product
ATLID	Atmospheric Lidar (on EarthCARE)
BBR	Broad-Band Radiometer (on EarthCARE)
CNN	Convolutional Neural Network
CPL	Cloud Physics Lidar
CPEX-CV	Convective Processes Experiment – Cabo Verde
CPR	Cloud Profiling Radar (on EarthCARE)
CRS	Cloud Radar System
CST	Combined System Test
DAAC	Distributed Active Archive Center
dBZ	decibels
DDA	Density Dimension Algorithm
DISC	EarthCARE Date Innovation and Science Cluster
DOE	Diffractive Optical Element
EarthCARE	Earth Cloud, Aerosol and Radiation Explorer
ECMWF	European Centre for Medium-Range Weather Forecasts
ECVT	EarthCARE Validation Team
eMAS	Enhanced MODIS Airborne Simulator
ER-2	Earth Resources-2 (NASA aircraft)
ESA	European Space Agency
GEOS-5	Goddard Earth Observing System Model, Version 5
GFS	Global Forecast System
GHz	Gigahertz
GLOVE	Goddard's Lidar Observation and Validation Experiment
GSFC	Goddard Space Flight Center
HSRL	High Spectral Resolution Lidar
ICESat-2	Ice, Cloud, and Land Elevation Satellite-2
IMPACTS	Investigation of Microphysics and Precipitation for Atlantic Coast-Threatening Snowstorms
JAXA	Japan Aerospace Exploration Agency
JMAG	EarthCARE Joint Mission Advisory Group
km	kilometers
LW	Longwave
LWIR	Longwave Infrared
m	meters
µm	microns
MERRA-2	Modern-Era Retrospective analysis for Research and Applications, Version 2
MODIS	Moderate-resolution Imaging Spectroradiometer
MSI	Multi-Spectral Imager (on EarthCARE)

Acronym	Definition
MTS	Mission Tools Suite
MWIR	Mid-Wave Infrared
NAM	North American Mesoscale (forecast system)
NASA	National Aeronautics and Space Administration
nm	nanometers
NPP	Suomi National Polar-orbiting Partnership
NWP	Numerical Weather Prediction
RADEX	Radar Definition Experiment
RGT	Reference Ground Track
s	seconds
SAFARI	Southern African Regional Science Initiative
SABRE	Stratospheric Aerosol processes, Budget and Radiative Effects
SEAC4RS	Studies of Emissions and Atmospheric Composition, Clouds, and Climate Coupling by Regional Surveys
SNR	Signal-to-Noise Ratio
sr	Steradians
SW	Shortwave
TC4	Tropical Composition Cloud and Climate Coupling
TOA	Top-of-Atmosphere
UTLS	Upper Troposphere-Lower Stratosphere
VIIRS	Visible Infrared Imaging Radiometer Suite
WH2yMSIE	Westcoast & Heartland Hyperspectral Microwave Sensor Intensive Experiment

Author contributions. The GLOVE field campaign is the product of a large team, many of whom are co-authors of this manuscript. JY led the creation of the manuscript and served as PI of GLOVE. EN served as GLOVE project scientist, led the coordination with the ECVT, and provide text for the manuscript. SP and KM served as leads for eMAS, providing text related to eMAS for the manuscript, Fig. 7, and participated in the field as mission scientists. MWM served as lead for CRS, providing text and figures related to CRS for the manuscript, while CH calibrated the CRS data. MK, KC, JF, NM, ED, and CH served as mission scientists in the field (performing flight planning and coordinated the campaign) and helped create Tables 4 and 5. JF and CH also provided meteorological support for field operations and provided text related to forecasting as well as input for Table 5. PS created Fig. 5. NRH provided Fig. 8, while MM provided the ICEsat-2 research product data to make Fig. 5. RK, JvB, and MPS were the GLOVE ECVT liasons, providing input to EarthCARE validation and providing preliminary EarthCARE data. All provided material for the manuscript and overall review.

Competing interests. The contact author has declared that none of the authors has any competing interests.

Disclaimer. Publisher's note: Copernicus Publications remains neutral with regard to jurisdictional claims made in the text, published maps, institutional affiliations, or any other geographical representation in this paper. The authors bear the ultimate responsibility for providing appropriate place names. Views expressed in the text are those of the authors and do not necessarily reflect the views of the publisher.

Acknowledgements. It takes many people to operate a field campaign. The authors would like to recognize the many people who made GLOVE a success, including: CPL team members Jennifer Moore, Amanda Cresanti; CRS team members Peter Pantina, Lihua Li, Gerry Heymsfield, and Skylar Hoffert; eMAS team members James Jacobson, Roseanne Dominguez, Gary Hoffmann, Ted Hildem, Nikolas Gibson, and Jeff Grose; Forecaster Stephen Nicholls; University of Iowa staff and students Joseph Gomes, Shi Kuang, Grant Finneman, and Jackson Begolka; all the NASA ER-2 pilots, navigators, staff, forecasters, and crew members.

Financial support. This research has been supported by the Division of Earth Sciences. GLOVE was funded by the ICESat-2 mission (Thorsten Markus, Tom Neumann, and Nathan Kurtz), NASA's Earth Science Research Program (Jack Kaye), NASA's Weather and Atmospheric Dynamics Research Program (Will McCarty), NASA's Radiation Sciences Program (Hal Maring).

Review statement. This paper was edited by Fan Mei and reviewed by Stefano Letizia and one anonymous referee.

References

Ackerman, A. S., Toon, O. B., Stevens, D. E., Heymsfield, A. J., Ramanathan, V., and Welton, E. J: Reduction of tropical cloudiness by soot, Science, 288, 1042–1047, 2000.

Ackerman, T. P., Kuo, N.-L., Valero, F. P. J., and Pfister, L.: Heating rates in tropical anvils, J. Atmos. Sci., 45, 1606–1623, 1988.

Albrecht, B. A.: Aerosols, cloud microphysics, and fractional cloudiness, Science, 245, 1227–1230, 1989.

Bruegge, C. J., Arnold, G. T., Czapla-Myers, J., Dominguez, R., Helmlinger, M. C., Thompson, D. R., Van den Bosch, J., and Wenny, B. N.: Vicarious Calibration of eMAS, AirMSPI, and AVIRIS Sensors During FIREX-AQ, IEEE T. Geosci. Remote Sens., 59, 10286–10297, https://doi.org/10.1109/TGRS.2021.3066997, 2021.

Chiriaco, M., Chepfer, H., Minnis, P., Haeffelin, M., Platnick, S., Baumgardner, D., Dubuisson, P., McGill, M., Noël, V., Pelon, J., Spangenberg, D., Sun-Mack, S., and Wind, G.: Comparison of CALIPSO-Like, LaRC, and MODIS Retrievals of Ice-Cloud Properties over SIRTA in France and Florida during CRYSTAL-FACE, J. Atmos. Ocean. Tech., https://doi.org/10.1175/JAM2435.1, 2007.

Christian, K. E., Palm, S. P., Yorks, J. E., and Nowottnick, E. P.: Evaluation of ICESat-2 ATL09 Atmospheric Products Using CALIOP and MODIS Space-Based Observations, Remote Sens., 17, 482, https://doi.org/10.3390/rs17030482, 2025.

Colette, A., Favez, O., Meleux, F., Chiappini, L., Haeffelin, M., Morille, Y., and Rouïl, L.: Assessing in near real time the impact of the April 2010 Eyjafjallajökull ash plume on air quality, Atmos. Environ., 45, 1217–1221, 2011.

Donovan, D. P., van Zadelhoff, G.-J., and Wang, P.: The EarthCARE lidar cloud and aerosol profile processor (A-PRO): the A-AER, A-EBD, A-TC, and A-ICE products, Atmos. Meas. Tech., 17, 5301–5340, https://doi.org/10.5194/amt-17-5301-2024, 2024.

European Space Agency: EarthCARE ATLID ICE Level 2A (version BA), Earth Online [data set], https://doi.org/10.57780/eca-e25465f, 2025a.

European Space Agency: EarthCARE CPR CLD Level 2A (version BA), Earth Online [data set], https://doi.org/10.57780/eca-7d84adf, 2025b.

European Space Agency: EarthCARE BBR MSI RAD Level 2B (version BA), Earth Online [data set], https://doi.org/10.57780/eca-176429f, 2025c.

Finlon, J., McDonald, V., McMurdie, L., Garcia, V., DeLaFrance, A., and Maherndl, N.: IMPACTS Tools (v1.0.0), Zenodo [code], https://doi.org/10.5281/zenodo.15310597, 2025.

Gomes, J., McGill, M. J., Selmer, P. A., and Kuang, S.: A Deep Learning Approach to Lidar Signal Denoising and Atmospheric Feature Detection, Remote Sensing., 17, 4060, https://doi.org/10.3390/rs17244060, 2025.

Haywood, J. M. and Boucher, O.: Estimates of the direct and indirect radiative forcing due to tropospheric aerosols: A review, Rev. Geophys., 38, 513–543, 2000.

Hlavka, D. L., Yorks, J. E., Young, S. A., Vaughan, M. A., Kuehn, R. E., McGill, M. J., and Rodier, S. D.: Airborne validation of cirrus cloud properties derived from CALIPSO lidar measurements: Optical properties, J. Geophys. Res., 117, D09207, https://doi.org/10.1029/2011JD017053, 2012.

Illingworth, A. J., Barker, H. W., Beljaars, A., Ceccaldi, M., Chepfer, H., Clerbaux, N., Cole, J., Delanoë, J., Domenech, C., Donovan, D. P., and Fukuda, S.: The EarthCARE Satellite: The Next Step Forward in Global Measurements of Clouds, Aerosols, Precipitation, and Radiation, B. Am. Meteorol. Soc., 96, 1311–1332, 2015.

Jensen, E. J., Lawson, P., Baker, B., Pilson, B., Mo, Q., Heymsfield, A. J., Bansemer, A., Bui, T. P., McGill, M., Hlavka, D., Heymsfield, G., Platnick, S., Arnold, G. T., and Tanelli, S.: On the importance of small ice crystals in tropical anvil cirrus, Atmos. Chem. Phys., 9, 5519–5537, https://doi.org/10.5194/acp-9-5519-2009, 2009.

King, M. D., Menzel, W. P., Grant, P. S., Myers, J. S., Arnold, G. T., Platnick, S. E., Gumley, L. E., Tsay, S.-C., Moeller, C. C., Fitzgerald, M., Brown, K. S., and Osterwisch, F. G.: Airborne Scanning Spectrometer for Remote Sensing of Cloud, Aerosol, Water Vapor, and Surface Properties, J. Atmos. Ocean. Tech., 13, 777–794, https://doi.org/10.1175/1520-0426(1996)013<0777:ASSFRS>2.0.CO;2, 1996.

King, M. D., Tsay, S.-C., Ackerman, S. A., and Larsen, N. F.: Discriminating heavy aerosol, clouds, and fires during SCAR-B: Application of airborne multispectral MAS data, J. Geophys. Res.-Atmos., 103, 31989–31999, https://doi.org/10.1029/98JD01043, 1998.

King, M. D., Platnick, S., Moeller, C. C., Revercomb, H. E., and Chu, D. A.: Remote sensing of smoke, land, and clouds from the NASA ER-2 during SAFARI 2000, J. Geophys. Res.-Atmos., 108, https://doi.org/10.1029/2002JD003207, 2003.

King, M. D., Platnick, S., Yang, P., Arnold, G. T., Gray, M. A., Riedi, J. C., Ackerman, S. A., and Liou, K.-N.: Remote Sensing of Liquid Water and Ice Cloud Optical Thickness and Effective Radius in the Arctic: Application of Airborne Multispectral MAS Data, J. Atmos. Ocean. Tech., 21, 857–875, https://doi.org/10.1175/1520-0426(2004)021<0857:RSOLWA>2.0.CO;2, 2004.

King, M. D., Platnick, S., Wind, G., Arnold, G. T., and Dominguez, R. T.: Remote sensing of radiative and microphysical properties of clouds during TC4: Results from MAS, MASTER, MODIS, and MISR, J. Geophys. Res., 115, 2009JD013277, https://doi.org/10.1029/2009JD013277, 2010.

Li, L., Heymsfield, G. M., Racette, P. E., Tian, L., and Zenker, E.: A 94-GHz cloud radar system on a NASA high-altitude ER-2 aircraft, J. Atmos. Ocean. Tech., 21, 1378–1388, 2004.

Li, L., Heymsfield, G. M., Tian, L., and Racette, P. E.: Measurements of Ocean Surface Backscattering Using an Airborne 94-GHz Cloud Radar – Implication for Calibration of Airborne and Spaceborne W-Band Radars, J. Atmos. Ocean. Tech., 22, 1033–1045, https://doi.org/10.1175/JTECH1722.1, 2005.

Liu, Z., McGill, M., Hu, Y., Hostetler, C. A., Vaughan, M., and Winker, D.: Validating lidar depolarization calibration using solar radiation scattered by ice clouds, Geoscience Remote Sens. Lett., 1, https://doi.org/10.1109/LGRS.2004.829613, 2004.

Markus, T., Neumann, T., Martino, A., Abdalati, W., Brunt, K., Csatho, B., Farrell, S., Fricker, H., Gardner, A., Harding, D., and Jasinski, M.: The Ice, Cloud, and land Elevation Satellite-2 (ICESat-2): Science requirements, concept, and implementation, Remote Sens. Environ., 190, 260–273, 2017.

Mason, S. L., Barker, H. W., Cole, J. N. S., Docter, N., Donovan, D. P., Hogan, R. J., Hünerbein, A., Kollias, P., Puigdomènech

Treserras, B., Qu, Z., Wandinger, U., and van Zadelhoff, G.-J.: An intercomparison of EarthCARE cloud, aerosol, and precipitation retrieval products, Atmos. Meas. Tech., 17, 875–898, https://doi.org/10.5194/amt-17-875-2024, 2024.

Mathur, R.: Estimating the impact of the 2004 Alaskan forest fires on episodic particulate matter pollution over the eastern United States through assimilation of satellite-derived aerosol optical depths in a regional air quality model, J. Geophys. Res.-Atmos., 113, https://doi.org/10.1029/2007JD009767, 2008.

McCorkel, J., Cairns, B., and Wasilewski, A.: Imager-to-radiometer in-flight cross calibration: RSP radiometric comparison with airborne and satellite sensors, Atmos. Meas. Tech., 9, 955–962, https://doi.org/10.5194/amt-9-955-2016, 2016.

McFarquhar, G. M., Heymsfield, A. J., Spinhirne, J., and Hart, B.: Thin and Subvisual Tropopause Tropical Cirrus: Observations and Radiative Impacts, J. Atmos. Sci., 57, 1841–1853, 2000.

McGill, M., Hlavka, D., Hart, W., Scott, V. S., Spinhirne, J., and Schmid, B.: Cloud physics lidar: Instrument description and initial measurement results, Appl. Optics, 41, 3725–3734, 2002.

McGill, M. J., Hlavka, D. L., Hart, W. D., Welton, E. J., and Campbell, J. R.: Airborne lidar measurements of aerosol optical properties during SAFARI-2000, J. Geophys. Res.-Atmos., 108, https://doi.org/10.1029/2002JD002370, 2003.

McGill, M. J., Vaughan, M. A., Trepte, C. R., Hart, W. D., Hlavka, D. L., Winker, D. M., and Kuehn, R.: Airborne validation of spatial properties measured by the CALIPSO lidar, J. Geophys. Res.-Atmos., 112, https://doi.org/10.1029/2007JD008768, 2007.

Meyer, K., Platnick, S., Arnold, G. T., Holz, R. E., Veglio, P., Yorks, J., and Wang, C.: Cirrus cloud optical and microphysical property retrievals from eMAS during SEAC^{4}RS using bi-spectral reflectance measurements within the 1.88 µm water vapor absorption band, Atmos. Meas. Tech., 9, 1743–1753, https://doi.org/10.5194/amt-9-1743-2016, 2016.

Meyer, K., Platnick, S., Arnold, G. T., Amarasinghe, N., Miller, D., Small-Griswold, J., Witte, M., Cairns, B., Gupta, S., McFarquhar, G., and O'Brien, J.: Evaluating spectral cloud effective radius retrievals from the Enhanced MODIS Airborne Simulator (eMAS) during ORACLES, Atmos. Meas. Tech., 18, 981–1011, https://doi.org/10.5194/amt-18-981-2025, 2025a.

Meyer, K., Platnick, S., Jacobson, J., Dominguez, R., Hildum, T., Gibson, N., Grose, J., Fraim, E., Arnold, G. T., and Yorks, J.: GSFC Lidar Observation and Validation Experiment (GLOVE) Enhanced MODIS Airborne Simulator (eMAS) Level-1B Version 2.0, NASA Level-1 and Atmosphere Archive & Distribution System (LAADS) Distributed Active Archive Center (DAAC) [data set], https://doi.org/10.5067/GLOVE/EMAS/EMASL1B.002, 2025b.

Miller, D. J., Sun, K., Zondlo, M. A., Kanter, D., Dubovik, O., Welton, E. J., and Ginoux, P.: Assessing boreal forest fire smoke aerosol impacts on US air quality: A case study using multiple data sets, J. Geophys. Res.-Atmos., 116, https://doi.org/10.1029/2011JD016170, 2011.

Nowottnick, E. P., Christian, K. E., Yorks, J. E., Midzak, N., Selmer, P. A., McGill, M. J., Lu, Z., Wang, J., and Salinas, S. V.: Aerosol Detection from the Cloud Aerosol Transport System on the International Space Station: Algorithm Overview and Implications for Diurnal Sampling, Atmosphere, 13, 1439, https://doi.org/10.3390/atmos13091439, 2022.

Oladipo, B., Gomes, J., McGill, M., and Selmer, P.: Leveraging Deep Learning as a New Approach to Layer Detection and Cloud–Aerosol Classification Using ICESat-2 Atmospheric Data, Remote Sens., 16, 2344, https://doi.org/10.3390/rs16132344, 2024.

Palm, S. P., Yang, Y., Herzfeld, U. C., Hancock, D., Barbieri, K. A., and Wimert, J.: ATLAS/ICESat-2 L3A Calibrated Backscatter Profiles and Atmospheric Layer Characteristics (ATL09, Version 1), NASA National Snow and Ice Data Center Distributed Active Archive Center [data set], https://doi.org/10.5067/ATLAS/ATL09.001, 2019.

Palm, S. P., Yang, Y., Herzfeld, U., Hancock, D., Hayes, A., Selmer, P., Hart, W., and Hlavka, D.: ICESat-2 Atmospheric Channel Description, Data Processing and First Results, Earth Space Sci., 8, e2020EA001470, https://doi.org/10.1029/2020EA001470, 2021.

Pauly, R. M., Yorks, J. E., Hlavka, D. L., McGill, M. J., Amiridis, V., Palm, S. P., Rodier, S. D., Vaughan, M. A., Selmer, P. A., Kupchock, A. W., Baars, H., and Gialitaki, A.: Cloud-Aerosol Transport System (CATS) 1064 nm calibration and validation, Atmos. Meas. Tech., 12, 6241–6258, https://doi.org/10.5194/amt-12-6241-2019, 2019.

Platnick, S., Durkee, P. A., Nielsen, K., Taylor, J. P., Tsay, S. C., King, M. D., Ferek, R. J., Hobbs, P. V., and Rottman, J. W.: The role of background cloud microphysics in the radiative formation of ship tracks, J. Atmos. Sci., 57, 2607–2624, 2000.

Platnick, S., Li, J. Y., King, M. D., Gerber, H., and Hobbs, P. V.: A solar reflectance method for retrieving the optical thickness and droplet size of liquid water clouds over snow and ice surfaces, J. Geophys. Res.-Atmos., 106, 15185–15199, 2001.

Rajeevan, M. and Srinivasan, J.: Net cloud radiative forcing at the top of the atmosphere in the Asian region, J. Climate, 13, 650–657, 2000.

Rosenfeld, D., Rudich, Y., and Lahav, R.: Desert dust suppressing precipitation: A possible desertification feedback loop, P. Natl. Acad. Sci. USA, 98, 5975–5980, 2001.

Schmid, B., Redemann, J., Russell, P. B., Hobbs, P. V., Hlavka, D. L., McGill, M. J., Holben, B. N., Welton, E. J., Campbell, J. R., Torres, O., and Kahn, R. A.: Coordinated airborne, spaceborne, and ground-based measurements of massive thick aerosol layers during the dry season in southern Africa, J. Geophys. Res.-Atmos., 108, https://doi.org/10.1029/2002JD002297, 2003.

Selmer, P., Yorks, J. E., Nowottnick, E. P., Cresanti, A., and Christian, K. E.: A Deep Learning Lidar Denoising Approach for Improving Atmospheric Feature Detection, Remote Sens., 16, 2735, https://doi.org/10.3390/rs16152735, 2024.

Shi, Y. R., Levy, R. C., Remer, L. A., Mattoo, S., and Arnold, G. T.: Investigating the Spatial and Temporal Limitations for Remote Sensing of Wildfire Smoke Using Satellite and Airborne Imagers During FIREX-AQ, J. Geophys. Res.-Atmos., 129, e2023JD039085, https://doi.org/10.1029/2023JD039085, 2024.

Stephens, G. L.: Cloud feedbacks in the climate system: A critical review, J. Climate, 18, 237–273, 2005.

Twomey, S.: The influence of pollution on the shortwave albedo of clouds, J. Atmos. Sci., 34, 1149–1152, 1977.

Vaughan, M., Powell, K. A., Winker, D. M., Hostetler, C. A., Kuehn, R. E., Hunt, W. H., Getzewich, B. J., Young, S. A., Liu, Z., and McGill, M. J.: Fully automated detection of cloud and aerosol layers in the CALIPSO li-

dar measurements, J. Atmos. Ocean. Tech., 26, 2034–2050, https://doi.org/10.1175/2009JTECHA1228.1, 2009.

Walker McLinden, M. L., Li, L., Heymsfield, G. M., Coon, M., and Emory, A.: The NASA GSFC 94-GHz airborne solid-state cloud radar system (CRS), J. Atmos. Ocean. Tech., 38, 1001–1017, 2021.

Walker McLinden, M., Li, L., Heymsfield, G., Helms, C., Pantina, P., Hoffert, S., Coon, M., and Yorks, J.: Cloud Radar System (CRS) Radar Level 1B Data Products from the GLOVE Field Campaign (Level 1B Initial Release), Zenodo [data set], https://doi.org/10.5281/zenodo.17179580, 2025.

Wehr, T. (Ed.): EarthCARE Mission Requirements Document. Earth and Mission Science Division, European Space Agency, https://doi.org/10.5270/esa.earthcare-mrd.2006, 2006.

Wehr, T., Kubota, T., Tzeremes, G., Wallace, K., Nakatsuka, H., Ohno, Y., Koopman, R., Rusli, S., Kikuchi, M., Eisinger, M., Tanaka, T., Taga, M., Deghaye, P., Tomita, E., and Bernaerts, D.: The EarthCARE mission – science and system overview, Atmos. Meas. Tech., 16, 3581–3608, https://doi.org/10.5194/amt-16-3581-2023, 2023.

Yorks, J. E., Hlavka, D. L., Hart, W. D., and McGill, M. J.: Statistics of cloud optical properties from airborne lidar measurements, J. Atmos. Ocean. Tech., 28, 869–883, https://doi.org/10.1175/2011JTECHA1507.1, 2011a.

Yorks, J. E., Hlavka, D. L., Vaughan, M. A., McGill, M. J., Hart, W. D., Rodier, S., and Kuehn, R.: Airborne validation of cirrus cloud properties derived from CALIPSO lidar measurements: Spatial properties, J. Geophys. Res., 116, D19207, https://doi.org/10.1029/2011JD015942, 2011b.

Yorks, J. E., McGill, M. J., Palm, S. P., Hlavka, D. L., Selmer, P. A., Nowottnick, E., Vaughan, M. A., Rodier, S., and Hart, W. D.: An Overview of the CATS Level 1 Data Products and Processing Algorithms, Geophys. Res. Lett., 43, https://doi.org/10.1002/2016GL068006, 2016.

Yorks, J. E., Selmer, P. A., Kupchock, A., Nowottnick, E. P., Christian, K. E., Rusinek, D., Dacic, N., and McGill, M. J.: Aerosol and Cloud Detection Using Machine Learning Algorithms and Space-Based Lidar Data, Atmosphere, 12, 606, https://doi.org/10.3390/atmos12050606, 2021.

Yorks, J., Selmer, P., Moore, J., Christian, K., Midzak, N., Finlon, J., Cresanti, A., Kuang, S., Finneman, G., Begolka, J., McGill, M., and Nowottnick, E.: Cloud Physics Lidar Level 1 & 2 Data Products from the GLOVE Field Campaign (Version 1), Zenodo [data set], https://doi.org/10.5281/zenodo.16807221, 2025.